# EM Scattering by a Conducting Sphere Coated with a Uniaxial Layer under Arbitrary Illumination Angle in a Fixed Laboratory Frame

*Yan SONG, Chun-Ming TSE*

Dept. of Electrical & Computer Engineering, National University of Singapore, 4 Engineering Drive 3, Singapore 117576

ricksong09@gmail.com, realzchun@gmail.com

**Abstract.** *Under a fixed laboratory frame, the electromagnetic theory of the scattering of a plane wave of arbitrary polarizations incidence from arbitrary angles by a uniaxial anisotropic medium was obtained for the first time, and could be solved analytically from an eigensystem determined by a uniaxial anisotropic medium. By applying the boundary conditions at respective interfaces of the coated spherical structure, the unknown expansion coefficients can be obtained from the incident field and the electromagnetic fields in the anisotropic medium, and from the scattered field. Not only did the numerical results demonstrate the validity of our proposed theory but this paper shall also provide discussions in relation to some general cases (under arbitrary incident angles) of bistatic radar cross section.*

## Keywords

Electromagnetic scattering, radar cross section (RCS), uniaxial anisotropic media, perfect electric conductor (PEC), spherical vector function, incident angle, azimuthal angle, axial ratio.

## 1. Introduction

In the past century, the electromagnetic scattering theory has been developed by Lorenz and Mie [1], [2], respectively, however the Mie theory continues to be further extended [3], [4]. In the existing works, many numerical and theoretical analytical methods have been established and developed over the past few decades, for example, Fourier transform [5], [6], spherical wave function expansion [7] and dyadic Green's functions [8], [9]. The solutions to the scattering problem of a conducting sphere have been discussed in the existing literature [10], and most methods can only present the incoming wave's propagation along the z-axis (or another fixed direction). However, in practice, the incident wave can come from any direction with respect to our fixed observation coordinate. In this paper, a derivation of a Mie-type solution to this problem of the scattering was obtained successfully. Our work provides a general and analytical scattering method for a uniaxial-coated perfect electric conductor (PEC) sphere under an illumination at any incident angle and azimuthal angle, whilst keeping a fixed laboratory frame for observing the radar cross section (RCS). After the results were validated by comparison with the existing data, some new numerical results are presented and discussed.

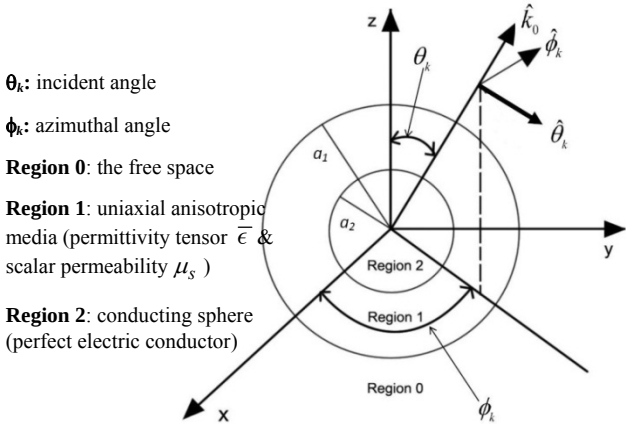


**Fig. 1.** The geometry of a conducting sphere coated with a uniaxial anisotropic media.

## 2. Formulation

Consider a conducting sphere coated with a shell made of uniaxial anisotropic medium illuminated by an incident wave. As shown in Fig. 1, a cross section of coated sphere with outer radius $a_1$ and inner radius $a_2$ is located at the coordinate origin. Three distinct regions are divided into, namely, region 0, region 1 and region 2. The uniaxial anisotropic with permittivity tensor $\bar{\epsilon}$ and scalar permeability $\mu_s$ are located with thickness ($a_1$-$a_2$). Assume that the incident electric field amplitude has unity of amplitude. The time dependence as exp(-$i\omega t$) is assumed but suppressed throughout the treatment.

The permittivity tensor of uniaxial anisotropic can be characterized by the following for arbitrary direction of propagation and polarization of the incident plane waves:

$$\bar{\epsilon} = \begin{bmatrix} \epsilon_s\epsilon_r & 0 & 0 \\ 0 & \epsilon_s\epsilon_r & 0 \\ 0 & 0 & \epsilon_s \end{bmatrix}. \tag{1}$$

The constitutive relations inside the uniaxial anisotropic medium can be expressed as:

$$\mathbf{D}_{\text{int}} = \bar{\epsilon} \cdot \mathbf{E}_{\text{int}}, \quad \mathbf{B}_{\text{int}} = \mu_s \cdot \mathbf{H}_{\text{int}} \tag{2}$$

The wave equation can be obtained as follows by substituting (2) into the sourceless Maxwell's equations.

$$\nabla \times \nabla \times (\epsilon_s \bar{\epsilon}^{-1} \cdot \mathbf{D}_{\text{int}}) - k_s^2 \mathbf{D}_{\text{int}} = 0 \tag{3}$$

where

$$\epsilon_s \bar{\epsilon}^{-1} = \begin{bmatrix} 1/\epsilon_r & 0 & 0 \\ 0 & 1/\epsilon_r & 0 \\ 0 & 0 & 1 \end{bmatrix}; k_s^2 = \omega^2 \epsilon_s \mu_s . \tag{4}$$

## 2.1 Expansion of Electromagnetic field inside Region 1(the uniaxial anisotropic medium)

$\mathbf{D}_{\text{int}}$ can be expanded in terms of vector spherical wave functions (VSWFs), we obtain

$$\begin{aligned} \mathbf{D}_{\text{int}} = \sum_{n,m} \bar{E}_{mn} [ & c_{mn} \mathbf{M}_{mn}^{(1)}(k,\mathbf{r}) + d_{mn} \mathbf{N}_{mn}^{(1)}(k,\mathbf{r}) \\ & + v_{mn} \mathbf{M}_{mn}^{(3)}(k,\mathbf{r}) + u_{mn} \mathbf{N}_{mn}^{(3)}(k,\mathbf{r})] \end{aligned} \tag{5.1}$$

where $k$ is as yet undetermined and $\bar{E}_{mn} = i^n E_0 C_{mn}$. $E_0$ is the amplitude of the incident electric field, where

$$C_{mn} = \left[ \frac{2n+1}{n(n+1)} \frac{(n-m)!}{(n+m)!} \right]^{\frac{1}{2}} \tag{5.2}$$

Unless explicitly specified, hereinafter $\sum_{m,n}$ implies that $n$ runs from 1 to $\infty$, and $m$ runs from $-n$ to $n$ for each $n$. In practice calculations, the expansion is uniformly convergent and can be truncated at $n=n_c=x+4x^{1/3}+2$ [11], size parameter $x=k_0 a_1$. With the use of the properties of VSWFs, we obtain

$$\epsilon_s \bar{\epsilon}^{-1} \mathbf{N}_{mn} = \sum_{v=0}^{+\infty} \sum_{u=-v}^{+v} [\bar{g}_{uv}^{mn} \mathbf{M}_{uv} + \bar{e}_{uv}^{mn} \mathbf{N}_{uv} + \bar{f}_{uv}^{mn} \mathbf{L}_{uv}] \tag{6.1}$$

$$\epsilon_s \bar{\epsilon}^{-1} \mathbf{M}_{mn} = \sum_{v=0}^{+\infty} \sum_{u=-v}^{+v} [\tilde{g}_{uv}^{mn} \mathbf{M}_{uv} + \tilde{e}_{uv}^{mn} \mathbf{N}_{uv} + \tilde{f}_{uv}^{mn} \mathbf{L}_{uv}] \tag{6.2}$$

where the coefficients $\bar{g}_{uv}^{mn}, \bar{e}_{uv}^{mn}, \bar{f}_{uv}^{mn}, \tilde{g}_{uv}^{mn}, \tilde{e}_{uv}^{mn}, \tilde{f}_{uv}^{mn}$ can be found in Appendix A. Substituting **(6)** into (5.1), one has

$$\begin{aligned} \epsilon_s \bar{\epsilon}^{-1} \cdot \mathbf{D}_{\text{int}} = & \sum_{n=1}^{+\infty} \sum_{m=-n}^{+n} \bar{E}_{mn} (\bar{c}_{mn} \mathbf{M}_{mn}^{(1)} + \bar{d}_{mn} \mathbf{N}_{mn}^{(1)} + \bar{w}_{mn} \mathbf{L}_{mn}^{(1)} + \\ & \bar{v}_{mn} \mathbf{M}_{mn}^{(3)} + \bar{u}_{mn} \mathbf{N}_{mn}^{(3)} + \bar{y}_{mn} \mathbf{L}_{mn}^{(3)}) + w_{00} \mathbf{L}_{00}^{(1)} + y_{00} \mathbf{L}_{00}^{(3)} \end{aligned} \tag{7}$$

The coefficients $\bar{c}_{mn}, \bar{d}_{mn}, \bar{w}_{mn}, \bar{v}_{mn}, \bar{u}_{mn}, \bar{y}_{mn}, w_{00}, y_{00}$ can be found in Appendix A.

Since VSWFs satisfy

$$\nabla \times \mathbf{M}_{mn} = k \mathbf{N}_{mn}, \nabla \times \mathbf{N}_{mn} = k \mathbf{M}_{mn}, \nabla \times \mathbf{L}_{mn} = 0 \tag{8}$$

Substituting (7) and (5.1) into (3) with simple manipulation, we obtain

$$\begin{aligned} & \sum_{n,m} \bar{E}_{mn} [\tilde{c}_{mn} \mathbf{M}_{mn}^{(1)}(k,\mathbf{r}) + \tilde{d}_{mn} \mathbf{N}_{mn}^{(1)}(k,\mathbf{r}) + \tilde{v}_{mn} \mathbf{M}_{mn}^{(3)}(k,\mathbf{r}) + \\ & \tilde{u}_{mn} \mathbf{N}_{mn}^{(3)}(k,\mathbf{r})] = 0 \end{aligned} \tag{9}$$

with

$$\tilde{d}_{mn} = k^2 \left[ \sum_{v,u} \frac{\bar{E}_{uv}}{\bar{E}_{mn}} (\bar{e}_{mn}^{uv} d_{uv} + \tilde{e}_{mn}^{uv} c_{uv}) \right] - k_s^2 d_{mn} \tag{10.1}$$

$$\tilde{c}_{mn} = k^2 \left[ \sum_{v,u} \frac{\bar{E}_{uv}}{\bar{E}_{mn}} (\bar{g}_{mn}^{uv} d_{uv} + \tilde{g}_{mn}^{uv} c_{uv}) \right] - k_s^2 c_{mn} \tag{10.2}$$

$$\tilde{u}_{mn} = k^2 \left[ \sum_{v,u} \frac{\bar{E}_{uv}}{\bar{E}_{mn}} (\bar{e}_{mn}^{uv} u_{uv} + \tilde{e}_{mn}^{uv} v_{uv}) \right] - k_s^2 u_{mn} \tag{10.3}$$

$$\tilde{v}_{mn} = k^2 \left[ \sum_{v,u} \frac{\bar{E}_{uv}}{\bar{E}_{mn}} (\bar{g}_{mn}^{uv} u_{uv} + \tilde{g}_{mn}^{uv} v_{uv}) \right] - k_s^2 v_{mn} \tag{10.4}$$

Equation (9) implies $\tilde{c}_{mn}$, $\tilde{d}_{mn}$, $\tilde{v}_{mn}$ and $\tilde{u}_{mn}$ equal to zero, thus they can be expressed in the matrix form and $\lambda = k_s^2 / k^2$;

$$\begin{pmatrix} \bar{\varepsilon} & \tilde{\varepsilon} & \bar{\varepsilon} & \tilde{\varepsilon} \\ \bar{\mathcal{G}} & \tilde{\mathcal{G}} & \bar{\mathcal{G}} & \tilde{\mathcal{G}} \end{pmatrix} \begin{pmatrix} d \\ c \\ u \\ v \end{pmatrix} = \lambda \begin{pmatrix} d \\ c \\ u \\ v \end{pmatrix} \tag{11.1}$$

The matrices are defined by the following

$$\bar{\mathcal{G}}_{mn,uv} = \frac{\bar{E}_{uv}}{\bar{E}_{mn}} \bar{g}_{mn}^{uv}; \bar{\varepsilon}_{mn,uv} = \frac{\bar{E}_{uv}}{\bar{E}_{mn}} \bar{e}_{mn}^{uv}; \tag{11.2}$$

$$\tilde{\mathcal{G}}_{mn,uv} = \frac{\bar{E}_{uv}}{\bar{E}_{mn}} \tilde{g}_{mn}^{uv}; \tilde{\varepsilon}_{mn,uv} = \frac{\bar{E}_{uv}}{\bar{E}_{mn}} \tilde{e}_{mn}^{uv}; \tag{11.3}$$

where $mn$ and $uv$ denoting the row and column indices, respectively. Equation (11.1) is an eigensystem with eigenvalue $\lambda_l$ and the eigenvectors $(d_{mn,l}, c_{mn,l})^{\mathrm{T}}$ where $l$ denotes the index of eigenvalues and corresponding eigenvectors. The new function $V_l$ can be constructed based on the eigenvectors:

$$\mathbf{V}_l = -i\frac{\epsilon_s}{\lambda_l}\sum_{n,m}\bar{E}_{mn}[c_{mn,l}\mathbf{M}^{(1)}_{mn}(k_l,\mathbf{r}) + d_{mn,l}\mathbf{N}^{(1)}_{mn}(k_l,\mathbf{r}) + v_{mn,l}\mathbf{M}^{(3)}_{mn}(k_l,\mathbf{r}) + u_{mn,l}\mathbf{N}^{(3)}_{mn}(k_l,\mathbf{r})] \quad (12)$$

where $k_l = k_s/\sqrt{\lambda_l}$;

Since $\nabla\cdot\mathbf{V}_l = 0$, (3) and (5) can be expressed as

$$\nabla\times\nabla\times(\epsilon_s\bar{\epsilon}^{-1}\cdot\mathbf{V}_l) - k_s^2\mathbf{V}_l = 0; \mathbf{D}_{\text{int}} = \sum_{l=1}^{2n_c(n_c+2)}\alpha_l\mathbf{V}_l \quad (13)$$

The expression coefficients $\alpha_l$ can be determined by matching boundary condition between the sphere and free space. $\mathbf{E}_{\text{int}}$ and $\mathbf{H}_{\text{int}}$ can be given by the following using (13).

$$\begin{aligned}\mathbf{E}_{\text{int}} &= \bar{\epsilon}^{-1}\cdot\mathbf{D}_{\text{int}}\\ &= -i\sum_{n,m}\bar{E}_{mn}\sum_l\alpha_l[c_{mn,l}\mathbf{M}^{(1)}_{mn}(k_l,\mathbf{r}) + d_{mn,l}\mathbf{N}^{(1)}_{mn}(k_l,\mathbf{r}) + \\ &\frac{\bar{w}_{mn,l}}{\lambda_l}\mathbf{L}^{(1)}_{mn}(k_l,\mathbf{r}) + v_{mn,l}\mathbf{M}^{(3)}_{mn}(k_l,\mathbf{r}) + u_{mn,l}\mathbf{N}^{(3)}_{mn}(k_l,\mathbf{r}) + \frac{\bar{y}_{mn,l}}{\lambda_l}\mathbf{L}^{(3)}_{mn}(k_l,\mathbf{r})]\\ &-i\sum_l\alpha_l\left[\frac{w_{00,l}}{\lambda_l}\mathbf{L}^{(1)}_{00}(k_l,\mathbf{r}) + \frac{y_{00,l}}{\lambda_l}\mathbf{L}^{(3)}_{00}(k_l,\mathbf{r})\right]\end{aligned} \quad (14)$$

$$\begin{aligned}\mathbf{H}_{\text{int}} &= -\frac{i}{\omega\mu_s}\nabla\times\mathbf{E}_{\text{int}}\\ &= -\sum_{n,m}\bar{E}_{mn}\sum_l\alpha_l\frac{k_l}{\mu_s\omega}[d_{mn,l}\mathbf{M}^{(1)}_{mn}(k_l,\mathbf{r}) + c_{mn,l}\mathbf{N}^{(1)}_{mn}(k_l,\mathbf{r})\\ &+u_{mn,l}\mathbf{M}^{(3)}_{mn}(k_l,\mathbf{r}) + v_{mn,l}\mathbf{N}^{(3)}_{mn}(k_l,\mathbf{r})]\end{aligned} \quad (15)$$

## 2.2 Expansion of Incident Field and Scattered Field

The incident fields are given as

$$\mathbf{E}_i = -\sum_{n,m}i\bar{E}_{mn}\left[p_{mn}\mathbf{N}^{(1)}_{mn}(k_0,\mathbf{r}) + q_{mn}\mathbf{M}^{(1)}_{mn}(k_0,\mathbf{r})\right] \quad (16.1)$$

$$\mathbf{H}_i = -\frac{k_0}{\mu_0\omega}\sum_{n,m}\bar{E}_{mn}\left[q_{mn}\mathbf{N}^{(1)}_{mn}(k_0,\mathbf{r}) + p_{mn}\mathbf{M}^{(1)}_{mn}(k_0,\mathbf{r})\right] \quad (16.2)$$

where expansion coefficients $p_{mn}$ and $q_{mn}$ are

$$p_{mn} = [p_\theta\tilde{\tau}_{mn}(\cos\theta_k) - ip_\phi\tilde{\pi}_{mn}(\cos\theta_k)]e^{-im\phi_k} \quad (17.1)$$

$$q_{mn} = [p_\theta\tilde{\pi}_{mn}(\cos\theta_k) - ip_\phi\tilde{\tau}_{mn}(\cos\theta_k)]e^{-im\phi_k} \quad (17.2)$$

The regular functions are given and defined in [11].

$$\tilde{\pi}_{mn}(\cos\theta) = C_{mn}\frac{m}{\sin\theta}P_n^m(\cos\theta) \quad (17.3)$$

$$\tilde{\tau}_{mn}(\cos\theta) = C_{mn}\frac{d}{d\theta}P_n^m(\cos\theta) \quad (17.4)$$

where $C_{mn}$ is given in (5.2).

The scattered fields are given explicitly as

$$\mathbf{E}_s = \sum_{n,m}i\bar{E}_{mn}\left[a_{mn}\mathbf{N}^{(3)}_{mn}(k_0,\mathbf{r}) + b_{mn}\mathbf{M}^{(3)}_{mn}(k_0,\mathbf{r})\right] \quad (18)$$

$$\mathbf{H}_s = \frac{k_0}{\mu_0\omega}\sum_{n,m}\bar{E}_{mn}\left[b_{mn}\mathbf{N}^{(3)}_{mn}(k_0,\mathbf{r}) + a_{mn}\mathbf{M}^{(3)}_{mn}(k_0,\mathbf{r})\right] \quad (19)$$

where $k_0^2 = \omega^2\epsilon_0\mu_0$.

The coefficients $a_{mn}$ and $b_{mn}$ can be determined by matching boundary condition between uniaxial anisotropic shell and free space.

## 2.3 Applying Boundary Conditions

When the boundary condition is applied on the surface of a conducting sphere (size parameters $x_0=k_0a_2$), the following equations can be obtained:

$$v_{mn,l} = -\frac{\psi_n(k_la_2)}{\xi_n(k_la_2)}c_{mn,l} = -\frac{1}{S_n(k_la_2)}c_{mn,l} \quad (20.1)$$

$$u_{mn,l} = -\frac{\psi_n'(k_la_2)}{\xi_n'(k_la_2)}d_{mn,l} = -\frac{1}{\bar{S}_n(k_la_2)}d_{mn,l} \quad (20.2)$$

$$\bar{y}_{mn,l} = -\frac{\psi_n(k_la_2)}{\xi_n(k_la_2)}\bar{w}_{mn,l} = -\frac{1}{S_n(k_la_2)}\bar{w}_{mn,l} \quad (20.3)$$

Similarly, when another boundary condition is applied at the interface between the free space and the uniaxial anisotropic shell (size parameter $x=k_0a_1$), we obtain

$$\left[\frac{\xi_n'(x)}{\psi_n'(x)}\right]a_{mn} + \sum_l\left[\frac{1}{m_s\bar{k}_l}\frac{\psi_n'(\bar{k}_lm_sx)}{\psi_n'(x)}d_{mn,l} + \frac{1}{m_s\bar{k}_l}\frac{\xi_n'(\bar{k}_lm_sx)}{\psi_n'(x)}u_{mn,l}\right]\alpha_l + \sum_l\left[\frac{1}{m_s\bar{k}_l\lambda_l}\frac{j_n(\bar{k}_lm_sx)}{\psi_n'(x)}\bar{w}_{mn,l} + \frac{1}{m_s\bar{k}_l\lambda_l}\frac{h_n^{(1)}(\bar{k}_lm_sx)}{\psi_n'(x)}\bar{y}_{mn,l}\right]\alpha_l = p_{mn} \quad (21.1)$$

$$\left[\frac{\xi_n(x)}{\psi_n(x)}\right]b_{mn} + \sum_l\left[\frac{1}{m_s\bar{k}_l}\frac{\psi_n(\bar{k}_lm_sx)}{\psi_n(x)}c_{mn,l} + \frac{1}{m_s\bar{k}_l}\frac{\xi_n(\bar{k}_lm_sx)}{\psi_n(x)}v_{mn,l}\right]\alpha_l = q_{mn} \quad (21.2)$$

$$\left[\frac{\xi_n(x)}{\psi_n(x)}\right]a_{mn} + \sum_l\left[\frac{\mu_0}{\mu_s}\frac{\psi_n(\bar{k}_lm_sx)}{\psi_n(x)}d_{mn,l} + \frac{\mu_0}{\mu_s}\frac{\xi_n(\bar{k}_lm_sx)}{\psi_n(x)}u_{mn,l}\right]\alpha_l = p_{mn} \quad (21.3)$$

$$\left[\frac{\xi_n'(x)}{\psi_n'(x)}\right]b_{mn} + \sum_l\left[\frac{\mu_0}{\mu_s}\frac{\psi_n'(\bar{k}_lm_sx)}{\psi_n'(x)}c_{mn,l} + \frac{\mu_0}{\mu_s}\frac{\xi_n'(\bar{k}_lm_sx)}{\psi_n'(x)}v_{mn,l}\right]\alpha_l + \sum_l\left[\frac{\mu_0}{\mu_s}\frac{j_n(\bar{k}_lm_sx)}{\psi_n'(x)}\bar{w}_{mn,l} + \frac{\mu_0}{\mu_s}\frac{h_n^{(1)}(\bar{k}_lm_sx)}{\psi_n'(x)}\bar{y}_{mn,l}\right]\alpha_l = q_{mn} \quad (21.4)$$

$\psi_n(z) = zj_n(z)$ and $\xi_n(z) = zh_n^{(1)}(z)$ are Riccati functions where $j_n(kr)$ and $h_n^{(1)}(kr)$ are the spherical Bessel functions of the first kind and third kind respectively [11].

Two new variables are introduced, namely

$$\Lambda_{mn,uv} = S_n(x)\delta_{nv}\delta_{mu}; \bar{\Lambda}_{mn,uv} = \bar{S}_n(x)\delta_{nv}\delta_{mu} \quad (22)$$

Thus,

$$U_{mn,l}=\frac{1}{m_s\bar{k}_l}T_n(x,\bar{k}_l m_s x)c_{mn,l}+\frac{1}{m_s\bar{k}_l}S_n(\bar{k}_l m_s x)T_n(x,\bar{k}_l m_s x)v_{mn,l} \tag{23.1}$$

$$\bar{U}_{mn,l}=\frac{1}{m_s\bar{k}_l}\bar{T}_n(x,\bar{k}_l m_s x)d_{mn,l}+\frac{1}{m_s\bar{k}_l}\bar{S}_n(\bar{k}_l m_s x)\bar{T}_n(x,\bar{k}_l m_s x)u_{mn,l}$$
$$+\frac{1}{m_s\bar{k}_l\lambda_l}\frac{1}{\bar{k}_l m_s x}\frac{\bar{T}_n(x,\bar{k}_l m_s x)}{D_n^{(1)}(\bar{k}_l m_s x)}\bar{\bar{w}}_{mn,l}+\frac{1}{m_s\bar{k}_l\lambda_l}\frac{1}{\bar{k}_l m_s x}\frac{S_n(\bar{k}_l m_s x)T_n(x,\bar{k}_l m_s x)}{D_n^{(1)}(\bar{k}_l m_s x)}\bar{\bar{y}}_{mn,l} \tag{23.2}$$

$$V_{mn,l}=\frac{\mu_0}{\mu_s}T_n(x,\bar{k}_l m_s x)\bar{d}_{mn,l}+\frac{\mu_0}{\mu_s}S_n(\bar{k}_l m_s x)T_n(x,\bar{k}_l m_s x)\bar{u}_{mn,l} \tag{23.3}$$

$$\bar{V}_{mn,l}=\frac{\mu_0}{\mu_s}\bar{T}_n(x,\bar{k}_l m_s x)\bar{c}_{mn,l}+\frac{\mu_0}{\mu_s}\bar{S}_n(\bar{k}_l m_s x)\bar{T}_n(x,\bar{k}_l m_s x)\bar{v}_{mn,l}$$
$$+\frac{\mu_0}{\mu_s}\frac{1}{\bar{k}_l m_s x}\frac{\bar{T}_n(x,\bar{k}_l m_s x)}{D_n^{(1)}(\bar{k}_l m_s x)}\bar{w}_{mn,l}+\frac{\mu_0}{\mu_s}\frac{1}{\bar{k}_l m_s x}\frac{S_n(\bar{k}_l m_s x)T_n(x,\bar{k}_l m_s x)}{D_n^{(1)}(\bar{k}_l m_s x)}\bar{y}_{mn,l} \tag{23.4}$$

where

$$m_s=\frac{k_s}{k_0};\bar{k}_l=\frac{k_l}{k_s} \tag{23.5}$$

$$S_n(n)=\frac{\xi_n(x)}{\psi_n(x)};\bar{S}_n(n)=\frac{\xi_n'(x)}{\psi_n'(x)};T_n(x,z)=\frac{\psi_n(z)}{\psi_n(x)};\bar{T}_n(x,z)=\frac{\psi_n'(z)}{\psi_n'(x)} \tag{23.6}$$

Logarithmic derivatives of Riccati-Bessel function [12] is

$$D_n^{(1)}(z)=\frac{\psi_n'(z)}{\psi_n(z)}$$

Equation (21) can be rewritten as

$$\bar{\Lambda}_{mn,uv}a_{mn}+\bar{U}_{mn,l}\tilde{\alpha}_l=p_{mn}, \tag{24.1}$$

$$\Lambda_{mn,uv}b_{mn}+V_{mn,l}\tilde{\alpha}_l=p_{mn}, \tag{24.2}$$

$$\Lambda_{mn,uv}a_{mn}+U_{mn,l}\tilde{\alpha}_l=q_{mn}, \tag{24.3}$$

$$\bar{\Lambda}_{mn,uv}b_{mn}+\bar{V}_{mn,l}\tilde{\alpha}_l=q_{mn} \tag{24.4}$$

Equation (24) can be represented as

$$\begin{pmatrix}\bar{\Lambda}&0\\0&\Lambda\end{pmatrix}\begin{pmatrix}a\\b\end{pmatrix}+\begin{pmatrix}\bar{U}\\U\end{pmatrix}\tilde{\alpha}_l=\begin{pmatrix}p\\q\end{pmatrix} \tag{25.1}$$

$$\begin{pmatrix}\Lambda&0\\0&\bar{\Lambda}\end{pmatrix}\begin{pmatrix}a\\b\end{pmatrix}+\begin{pmatrix}\bar{V}\\V\end{pmatrix}\tilde{\alpha}_l=\begin{pmatrix}p\\q\end{pmatrix} \tag{25.2}$$

Finally (25) can be solved

$$\tilde{\alpha}=\left[\begin{pmatrix}\bar{U}\\U\end{pmatrix}+\begin{pmatrix}\bar{\Lambda}&0\\0&\Lambda\end{pmatrix}\begin{pmatrix}\bar{\Lambda}-\Lambda&0\\0&\Lambda-\bar{\Lambda}\end{pmatrix}^{-1}\begin{pmatrix}V-\bar{U}\\\bar{V}-U\end{pmatrix}^{-1}\right]^{-1}\begin{pmatrix}p\\q\end{pmatrix} \tag{26}$$

$$\tilde{\alpha}=\Re\begin{pmatrix}p\\q\end{pmatrix};\begin{pmatrix}a\\b\end{pmatrix}=S\begin{pmatrix}p\\q\end{pmatrix} \tag{27}$$

$$\Re=\left[\begin{pmatrix}\bar{U}\\U\end{pmatrix}+\begin{pmatrix}\bar{\Lambda}&0\\0&\Lambda\end{pmatrix}Z\right]^{-1};Z=\begin{pmatrix}\gamma&0\\0&-\gamma\end{pmatrix}^{-1}\begin{pmatrix}V-\bar{U}\\\bar{V}-U\end{pmatrix} \tag{28}$$

$$S=Z\Re;\gamma=\bar{\Lambda}-\Lambda. \tag{29}$$

Thus the unknown coefficients of electromagnetic fields in the uniaxial anisotropic spherical medium can be obtained, and the coefficients of scattered fields in free space can be calculated using the aforementioned method. With the scattering coefficients obtained from (16) and (17), we obtain the radar cross section for the arbitrary incident angle.

$$\sigma=\lim_{r\to\infty}4\pi\frac{d\sigma_{sca}}{d\Omega},where\frac{d\sigma_{sca}}{d\Omega}=\left|\mathrm{f}(\theta,\phi)\right|^2 \tag{30}$$

$$\mathbf{E_s}=E_o\mathrm{f}(\theta,\varphi)\frac{e^{ik_0r}}{r},r\to\infty \tag{31}$$

where $d\sigma_{sca}/d\Omega$ is the differential scattering cross section and $\mathrm{f}(\theta,\phi)$ is the scattering amplitude.

## 3. Numerical Results and Discussion

The numerical results obtained are shown in this section for a conducting sphere coated with a shell made of uniaxial anisotropic material. Firstly, the results in this paper are compared with the existing works to verify our theory and its accuracy, and program codes.

Fig.2 (a) illustrates the result from [13] about the bistatic RCS by a conducting sphere coated with uniaxial anisotropic medium. This shows that the results in this paper agree with the existing works.

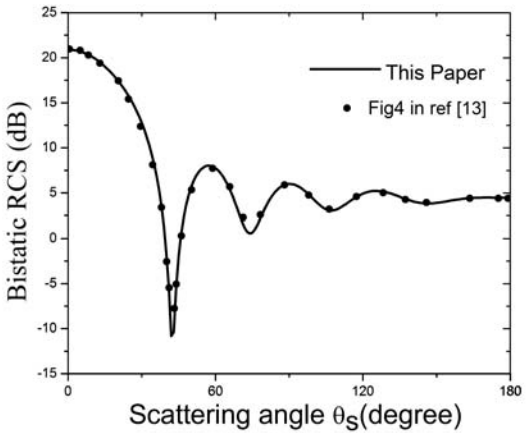


**Fig. 2.(a)** Bistatic RCS of the uniaxial anisotropic medium ($TiO_2$) coated sphere in the E plane with $k_0a_1=2\pi$ and $k_0a_2=1.6\pi$. The permittivity tensor is $\varepsilon_t\varepsilon_s=5.913\varepsilon_0$, $\varepsilon_s=7.197\varepsilon_0$, the incident wave propagates in $+\hat{z}$ direction.

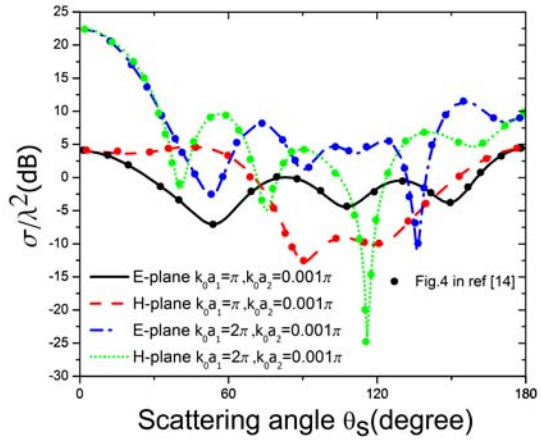


**Fig. 2.(b)** RCS versus the scattering angle in both the E-plane and the H-plane. The radius of conducting sphere is assumed to be extremely small ($k_0a_2$=0.001π) which tends to a homogenous uniaxial anisotropic sphere. The electric size of homogeneous uniaxial anisotropic sphere is chosen as $k_0a_1$=π and $k_0a_1$=2π respectively. The permittivity tensor elements are $\varepsilon_r\varepsilon_s$ = 5.3495, $\varepsilon_s$=4.9284$\varepsilon_0$.

Secondly, Geng et al [14] presented RCS for a general lossless uniaxial anisotropic medium. In Fig. 2 (b), it is seen apparently that RCS calculated by using our present method in this paper and the Fourier Transform method agrees excellently in both the E plane and the H plane. This agreement once again verifies the applicability of our theory and accuracy of the program codes developed.

Fig. 3(a) represents the radar cross-section at two incident angles with the same permittivity tensor. The radius of conducting sphere is assumed to be extremely small ($k_0a_2$=0.001π) which tends to a homogeneous uniaxial anisotropic sphere with ($k_0a_1$=π). It can be seen that the shape of cross section is similar as the incident angle varies. The maximum and minimum in the E plane scattering both increase and they move rightwards, but the maximum in the H plane scattering decreases and minimum increases as the incident angle increases. Fig. 3(b) shows the variation of the radar cross section at two incident angles in the uniaxial anisotropic-coated PEC sphere. It can be observed that there is a reduction in the E plane compared with Fig. 3(a) at $\theta_s$ = 105° and $\theta_s$ = 115°, respectively. As the incident angle is increased to 30°, it is noted that a good convergence at $\theta_s$ = 180° is increased to -2dB in the E plane and the H plane. Both the E-plane and H-plane in these two figures move towards the other end of the sphere as the incident angle increases.

Fig.4 illustrates the effect of anisotropic ratio on the RCS in both the E plane and the H plane. It is seen that the RCS in the E plane will have a great reduction at $\theta_s$ =112° as $\varepsilon_r$ increases and $\varepsilon_s$ remains constant, but RCS in the H plane will have a small rise at $\theta_s$ =112°. As $\varepsilon_r$ increases gradually, RCS in both the E plane and the H plane drops greatly at $\theta_s$ =180° and rises at $\theta_s$ =0°.

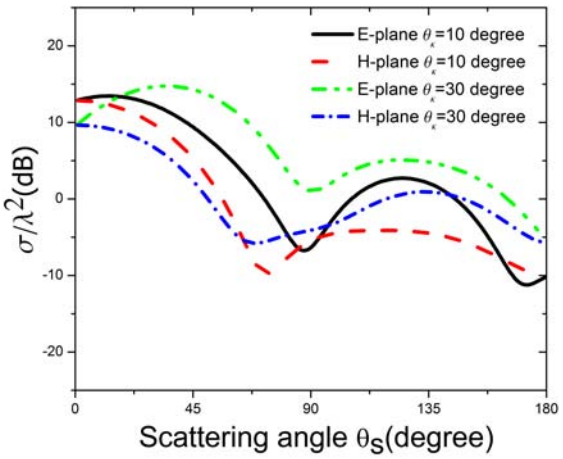


**Fig.3.** Radar cross-section (RCS) versus scattering angle at $\theta_k$ =10° and 30° in the E plane and the H plane and the permittivity tensors are assumed to be $\varepsilon_r\varepsilon_s$ =2$\varepsilon_0$, $\varepsilon_s$=4$\varepsilon_0$. **(a)** The electrical dimensions are $k_0a_1$=π and $k_0a_2$=0.001π.

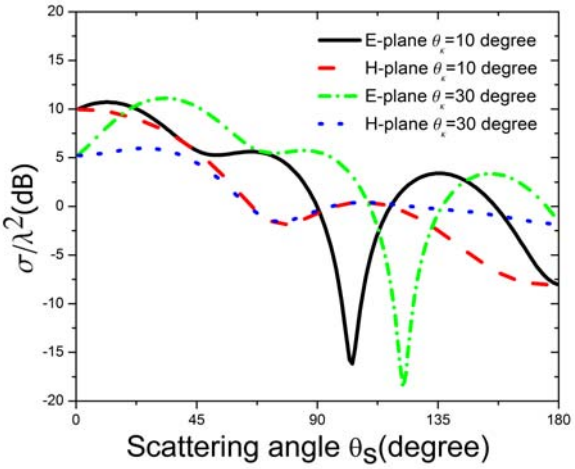


**Fig. 3.(b)** The electrical dimensions are $k_0a_1$=π and $k_0a_2$=0.9π.

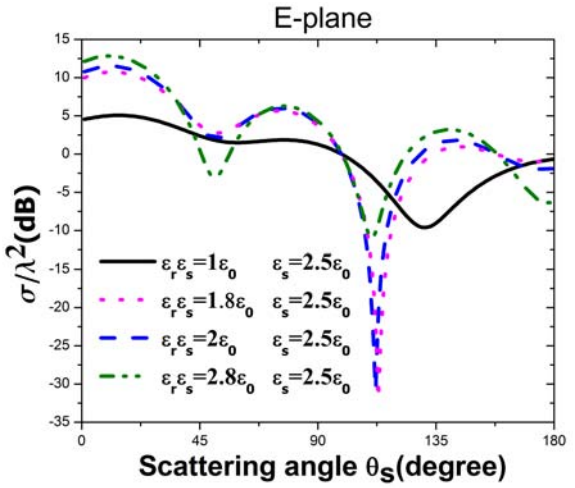


**Fig. 4.** Radar cross-section (RCS) versus scattering angle at $\theta_k$ =10°, $k_0a_1$ =π and $k_0a_2$ =0.75π. **(a)** In the E plane

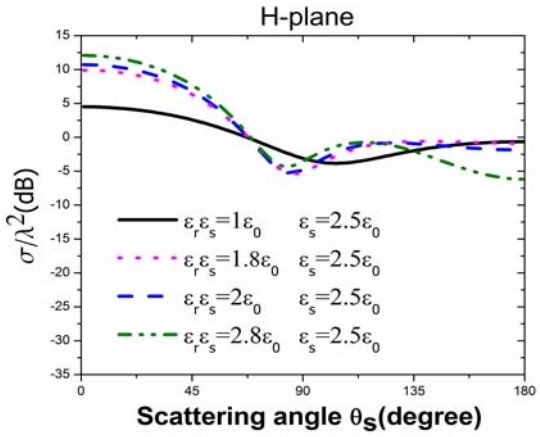


**Fig. 4. (b)** In the H plane.

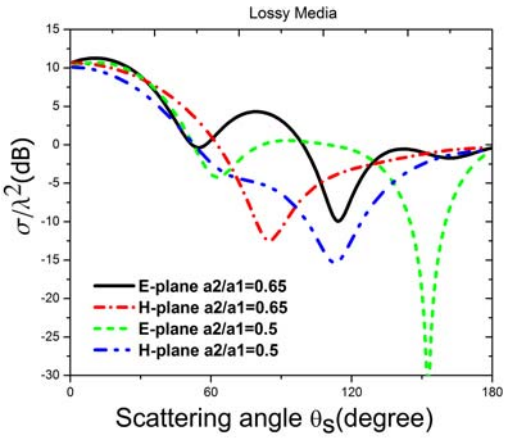


**Fig. 5.(a)** Radar cross section versus scattering angle at axial ratio $\eta = (a_2/a_1) = 0.65$ and 0.5 in lossy media. The permittivity tensor is assumed to be $\varepsilon_r\varepsilon_s = (4+0.2i)\varepsilon_0$, $\varepsilon_s = (2+0.1i)\varepsilon_0$, $k_0a_1 = \pi$ and the incident angle $\theta_k = 10^o$.

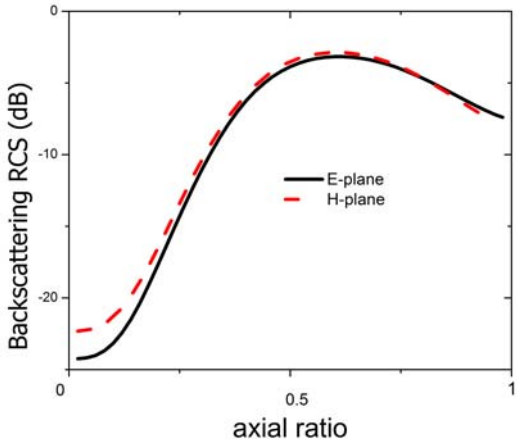


**Fig. 5.(b)** Backscattering radar cross section versus axial ratio range at $\theta_k = 10^o$. $\varepsilon_r\varepsilon_s = 2\varepsilon_0$, $\varepsilon_s = 4\varepsilon_0$. Size parameter at outer layer is chosen as $k_0a_1 = 0.5\pi$.

In Fig. 5(a), it is seen that the RCS reduces greatly in the E plane at $\theta_s = 152^o$ as axial ratio rises but a small drop occurs in the H plane at $\theta_s = 116^o$. A good convergence can be achieved at -1dB at $\theta_s = 180^o$. Fig. 5(b) shows backscattering RCS has the maximum in both the E plane and the H plane at axial ratio = 0.6. As the axial ratio starts from 0.6, backscattering RCS is decreasing.

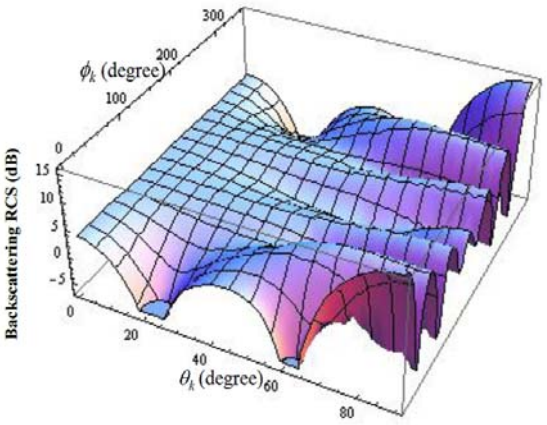


**Fig. 6.** The backscattering RCS versus any incident angle $\theta_k$ ($0^o$ to $90^o$) and azimuthal angle $\phi_k$ ($0^o$ to $360^o$) in 3D plot.

Fig.6 depicts the performance of backscattering RCS on variation of the incident angle and the azimuthal angle, $\varepsilon_r\varepsilon_s = 2\varepsilon_0$, $\varepsilon_s = 4\varepsilon_0$ and $k_0a_1 = \pi$ and $k_0a_2 = 0.5\pi$. It shows how the angles $\theta_k$ and $\phi_k$ influence the scattering cross section, which has never been reported. The backscatters are same at $\theta_k = 0^o$ as azimuthal angle $\phi_k$ varies from $0^o$ to $360^o$ but a greater variation of backscattering will be observed as the incident angle $\theta_k$ increases gradually to $90^o$.

## 4. Conclusion

In this paper, the problem of electromagnetic scattering by a conducting sphere coated with a uniaxial anisotropic layer has been successfully modeled and solved using the mode expansion method. This analytical approach may be used for electromagnetic scattering and controlling of radar cross section (RCS) by manipulating the anisotropy and illumination angle, which can only be analytically treated by our approach so far. For example, in the radar detection, the scattering by an object was calculated under fixed radar wave incident direction in the existing works. However, this is a shortcoming to the radar detection system in practice since the radar wave may be incident upon a target from any direction. Therefore, our work provides an analytical solution to characterize the scattering feature of the target and predict the scattered power around the target from any incident angle, which will be useful in reconstructing the radar image of the object more accurately. On the other hand, given that a radar wave illuminates an anisotropic object, our method can also be used to maximize or minimize the scattering by positioning the anisotropic object since the scattering heavily relies on the anisotropy and the incident angle. The present method might be further extended to a variety of applications in target shielding studies, microwave devices and also help in understanding wireless communication channels.

# Appendix

VSWFs are given by [11]

$$\mathbf{M}_{mn}^{(J)}(k,\mathbf{r})=\left[i\pi_{mn}(\cos\theta)e_{\theta}-\tau_{mn}(\cos\theta)e_{\phi}\right]z_n^{(J)}(kr)e^{im\phi} \tag{A-1a}$$

$$\mathbf{N}_{mn}^{(J)}(k,\mathbf{r})=\left[\tau_{mn}(\cos\theta)e_{\theta}-i\pi_{mn}(\cos\theta)e_{\phi}\right]\frac{1}{kr}\frac{d}{dr}\left[rz_n^{(J)}(kr)\right]\times e^{im\phi}$$
$$+e_r n(n+1)P_n^m(\cos\theta)\frac{z_n^{(J)}(kr)}{kr}e^{im\phi} \tag{A-1b}$$

$$\mathbf{L}_{mn}^{(J)}(k,\mathbf{r})=\left[\tau_{mn}(\cos\theta)e_{\theta}-i\pi_{mn}(\cos\theta)e_{\phi}\right]\frac{z_n^{(J)}(kr)}{kr}e^{im\phi}$$
$$+e_r P_n^m(\cos\theta)\frac{1}{kr}\frac{d}{dr}\left[rz_n^{(J)}(kr)\right]e^{im\phi} \tag{A-1c}$$

Two auxiliary functions are shown

$$\pi_{mn}(\cos\theta)=\frac{m}{\sin\theta}P_n^m(\cos\theta);\tau_{mn}(\cos\theta)=\frac{d}{d\theta}P_n^m(\cos\theta) \tag{A-2}$$

The coefficients in (6) are given

$$\tilde{g}_{uv}^{mn}=\delta_{nv}\delta_{mu}+\left[\frac{(n^2+n-m^2)(1/\epsilon_r-1)}{n(n+1)}\right]\delta_{nv}\delta_{mu} \tag{A-3a}$$

$$\tilde{e}_{uv}^{mn}=\frac{i(n+m)\left[m(1/\epsilon_r-1)\right]\delta_{n-1,v}\delta_{mu}}{n(2n+1)}+\frac{i(n-m+1)\left[m(1/\epsilon_r-1)\right]\delta_{n+1,v}\delta_{mu}}{(n+1)(2n+1)} \tag{A-3b}$$

$$\tilde{f}_{uv}^{mn}=\frac{-i(n+m)\left[m(1/\epsilon_r-1)\right]\delta_{n-1,v}\delta_{mu}}{2n+1}+\frac{i(n-m+1)\left[m(1/\epsilon_r-1)\right]\delta_{n+1,v}\delta_{mu}}{(n+1)(2n+1)} \tag{A-3c}$$

$$\bar{g}_{uv}^{mn}=\frac{-i(n+m)(n+1)\left[m(1/\epsilon_r-1)\right]\delta_{n-1,v}\delta_{mu}}{n(n-1)(2n+1)}$$
$$-\frac{i(n-m+1)n\left[m(1/\epsilon_r-1)\right]\delta_{n+1,v}\delta_{mu}}{(n+1)(n+2)(2n+1)} \tag{A-3d}$$

$$\bar{e}_{uv}^{mn}=\frac{[(2n^2+2n-3)m^2+(2n^2+2n-3)n(n+1)](1/\epsilon_r-1)}{n(n+1)(2n-1)(2n+3)}\delta_{nv}\delta_{mu}$$
$$+\delta_{nv}\delta_{mu}-\frac{(n+1)(n+m-1)(n+m)(1/\epsilon_r-1)\delta_{n-2,v}\delta_{mu}}{(n+1)(2n-1)(2n+3)}$$
$$-\frac{n(n-m+1)(n-m+2)(1/\epsilon_r-1)\delta_{n+2,v}\delta_{mu}}{(n+2)(2n+1)(2n+3)} \tag{A-3e}$$

$$\bar{f}_{uv}^{mn}=-\frac{(n^2+n-3m^2)(1/\epsilon_r-1)}{(2n-1)(2n+3)}\delta_{nv}\delta_{mu}$$
$$+\frac{(n+1)(n+m-1)(n+m)(1/\epsilon_r-1)\delta_{n-2,v}\delta_{mu}}{(2n-1)(2n+1)}$$
$$-\frac{n(n-m+1)(n-m+2)(1/\epsilon_r-1)\delta_{n+2,v}\delta_{mu}}{(2n+1)(2n+3)} \tag{A-3f}$$

The coefficients in (7) are shown

$$\bar{c}_{mn}=\sum_{v,u}\frac{\bar{E}_{uv}}{\bar{E}_{mn}}(\tilde{g}_{mn}^{uv}c_{uv}+\bar{g}_{mn}^{uv}d_{uv});\bar{d}_{mn}=\sum_{v,u}\frac{\bar{E}_{uv}}{\bar{E}_{mn}}(\tilde{e}_{mn}^{uv}c_{uv}+\bar{e}_{mn}^{uv}d_{uv}) \tag{A-4a}$$

$$\bar{w}_{mn}=\sum_{v,u}\frac{\bar{E}_{uv}}{\bar{E}_{mn}}(\tilde{f}_{mn}^{uv}c_{uv}+\bar{f}_{mn}^{uv}d_{uv});\bar{u}_{mn}=\sum_{v,u}\frac{\bar{E}_{uv}}{\bar{E}_{mn}}(\tilde{g}_{mn}^{uv}v_{uv}+\bar{g}_{mn}^{uv}u_{uv}) \tag{A-4b}$$

$$\bar{v}_{mn}=\sum_{v,u}\frac{\bar{E}_{uv}}{\bar{E}_{mn}}(\tilde{e}_{mn}^{uv}v_{uv}+\bar{e}_{mn}^{uv}u_{uv});\bar{y}_{mn}=\sum_{v,u}\frac{\bar{E}_{uv}}{\bar{E}_{mn}}(\tilde{f}_{mn}^{uv}v_{uv}+\bar{f}_{mn}^{uv}u_{uv}) \tag{A-4c}$$

$$w_{00}=\sum_{v,u}\frac{\bar{E}_{uv}}{\bar{E}_{mn}}(\tilde{f}_{mn}^{uv}c_{uv}+\bar{f}_{mn}^{uv}d_{uv})=(\frac{2}{15})^{\frac{1}{2}}\left(1/\epsilon_r-1\right)d_{02}E_0 \tag{A-4d}$$

$$y_{00}=\sum_{v,u}\frac{\bar{E}_{uv}}{\bar{E}_{mn}}(\tilde{f}_{mn}^{uv}v_{uv}+\bar{f}_{mn}^{uv}u_{uv})=(\frac{2}{15})^{\frac{1}{2}}\left(1/\epsilon_r-1\right)v_{02}E_0 \tag{A-4e}$$

VSWFs when $r\to\infty$ [15]

$$\mathbf{M}_{mn}^{(3)}=(-i)^n\left[\pi_{mn}(\cos\theta)e_{\phi}+i\tau_{mn}(\cos\theta)e_{\theta}\right]\frac{e^{ix}}{x}e^{im\phi} \tag{A-5a}$$

$$\mathbf{N}_{mn}^{(3)}=(-i)^n\left[\tau_{mn}(\cos\theta)e_{\theta}+i\pi_{mn}(\cos\theta)e_{\phi}\right]\frac{e^{ix}}{x}e^{im\phi} \tag{A-5b}$$

# References


[1] KONG, J. A. *Electromagnetic Wave Theory*. Cambrige, MA: EMW Publishing, 2005.

[2] MIE, D. Beitrage zur Optik truber Medien speziell kolloidaler Metallosungen. *Ann.Phys*., 1908, vol. 25, p. 377-455.

[3] ADEN, A. L., M. KERKER, M. Scattering of electromagnetic wave from two concentric spheres. *J. Appl. Phys*. 1951, vol. 22, p. 1242-1246.

[4] KEENER, J. D., CHALUT, K. J., PYHTILA, J. W., WAX, A. Application of Mie theory to determine the structure of spheroidal scatterers in biological materials. *Opt. Lett.*, 2007, vol. 32, no. 10, p. 1326-1328.

[5] GENG, Y. L., QIU, C.-W., YUAN, N. Exact solution to electromagnetic scattering by an impedance sphere coated with a uniaxial anisotropic layer. *IEEE Trans. Antennas Propagat*, 2009, vol. 57, no. 2, p. 572-576.

[6] GENG, Y. L., QIU, C.-W., ZOUHDI, S. Full-wave analysis of extraordinary backscattering by a layered plasmonic nanosphere. *J. Appl. Phys.*, 2008, vol. 104, 034909.

[7] LIN, Z., CHUI, S. T. Electromagnetic scattering by optically anisotropic magnetic particle. *Physical Review E,* 2004, vol. 69, 056614.

[8] QIU, C.-W., LI, L. W., ZOUHDI, S., YEO, T. S., WU, Q. On the integral identities consisting of two spherical Bessel functions. *IEEE Trans. Antennas Propagat*, 2007, vol. 55, no. 1, p. 240-244.

[9] QIU, C.W., ZOUHDI, S., RAZEK, A. Modified spherical wave functions with anisotropy ratio: Application to the analysis of scattering by multilayered anisotropic shells. *IEEE Trans Antennas Propagat*, 2007, vol. 55, no. 12, p. 3515-3523.

[10] RICHMOND, J. H. Scattering by a ferrite-coated conducting sphere. *IEEE Trans. Antennas Propag*., 1987, vol. 35, p. 73–79.

[11] BOHREN, C. F., HUFFMAN, D. R. *Absorption and Scattering of Light by Small Particles*. New York: Wiley, 1983.

[12] QIU, C. W., LI, L. W., YEO, T. S., ZOUHDI, S. Scattering by rotationally symmetric anisotropic spheres: Potential formulation and parametric studies*., Phys. Rev. E*, 2007, vol. 75, 026609.

[13] LV, C. J., SHI, Y., LIANG, C. H. Higher order hierarchical Legendre basis functions application to the analysis of scattering by uniaxial anisotropic objects. *Progress in Electromagnetics Research*, 2010, vol .13, p133-143.

[14] GENG, Y. L., WU, X. B., LI, L. W., GUAN, B. R. Mie scattering by a uniaxial anisotropic sphere. *Phys. Rev. E,* 2004, vol. 70, no. 5, p. 056609.

[15] YU-LIN XU Electromagnetic scattering by an aggregate of spheres: Far field. *Applied Optics*, December 1997, vol. 36, no 36, p. 9496-9508.